

Study of point- and cluster-defects in radiation-damaged silicon

Elena M. Donegani¹, Eckhart Fretwurst¹, Erika Garutti¹, Robert Klanner^{1*},
Gunnar Lindstroem¹, Ioana Pintilie², Roxana Radu², Joern Schwandt¹

¹*Institute for Experimental Physics, University of Hamburg, Luruper Chaussee 149, 22761 Hamburg, Germany*

²*National Institute of Material Physics, Magurele, Romania*

Abstract

Non-ionising energy loss of radiation produces point defects and defect clusters in silicon, which result in a significant degradation of sensor performance. In this contribution results from TSC (Thermally Stimulated Current) defect spectroscopy for silicon pad diodes irradiated by electrons to fluences of a few 10^{14} cm^{-2} and energies between 3.5 and 27 MeV for isochronal annealing between 80 and 280 °C, are presented. A method based on SRH (Shockley-Read-Hall) statistics is introduced, which assumes that the ionisation energy of the defects in a cluster depends on the fraction of occupied traps. The difference of ionisation energy of an isolated point defect and a fully occupied cluster, ΔE_a , is extracted from the TSC data.

For the VO_i (vacancy-oxygen interstitial) defect $\Delta E_a = 0$ is found, which confirms that it is a point defect, and validates the method for point defects. For clusters made of deep acceptors the ΔE_a values for different defects are determined after annealing at 80 °C as a function of electron energy, and for the irradiation with 15 MeV electrons as a function of annealing temperature. For the irradiation with 3.5 MeV electrons the value $\Delta E_a = 0$ is found, whereas for the electron energies of 6 to 27 MeV $\Delta E_a > 0$. This agrees with the expected threshold of about 5 MeV for cluster formation by electrons. The ΔE_a values determined as a function of annealing temperature show that the annealing rate is different for different defects. A naive diffusion model is used to estimate the temperature dependencies of the diffusion of the defects in the clusters.

Keywords: Silicon detectors, radiation damage, Shockley-Reed-Hall statistics, point defects, cluster defects, defect diffusion

Contents

1	Introduction	2
2	Test Structures and Measurements	2
3	Analysis Method	3
4	Results	5
4.1	The VO_i defect	5
4.2	Cluster defects	6
4.3	Cluster annealing	8
5	Conclusions	12
6	Acknowledgements	12
7	References	13

*Corresponding author. Email: Robert.Klanner@desy.de. Telephone: +49 40 8998 2558.

1. Introduction

Bulk-radiation damage in silicon limits the use of silicon detectors in high-radiation environments like at the CERN-LHC or in space. Although both microscopic and macroscopic effects of bulk damage are qualitatively understood, in spite of claims to the contrary, a consistent quantitative description of the data available has not yet been achieved. However, this is required for reliably predicting the sensor performance as a function of particle type and fluence, sensor design and operating parameters. The reason is that the number of radiation-induced states in the silicon band gap is large (see figure 1), their properties are frequently only poorly known, and *effective states* [1] have to be used in simulations because of the large number of defects. In addition, a quantitative understanding of defect clusters is lacking and in the TCAD simulations they are approximated by point defects.

In this contribution we propose a simple, physics motivated parametrization of the properties of cluster defects and apply it to spectroscopic results from TSC (Thermally Stimulated Current) measurements. We present results for silicon irradiated with electrons of 3.5 to 27 MeV kinetic energy [2, 3]. As the threshold for defect cluster production is expected to be around 5 MeV for electrons [4], these data are well suited to check the validity of the method.

In the present work single vacancy related defects are considered to be point-like defects (e. g. the VO_i defect). Such isolated point defects are produced in silicon by low energy recoils, whereas an agglomeration of defects (or a cluster for short) results from high energy recoils that introduce a dense cascade of silicon atoms displaced from their original lattice position.

2. Test Structures and Measurements

For the studies p^+n^+ pad diodes, produced on 283 μm thick float-zone n-type silicon with a phosphorous-doping of approximately 10^{12} cm^{-3} and an oxygen concentration $< 10^{16} \text{ cm}^{-3}$, were used. The p^+ implant of 25 mm^2 area is surrounded by a guard ring. A window in the aluminum on top of the p^+ implant with the shape of a decagon and an area of 3.25 mm^2 allows to inject light through the p^+ contact. The n^+ back contact is covered by an aluminum grid.

The pad diodes have been irradiated with electrons of $E_e = 3.5, 6, 15,$ and 27 MeV to fluences between 1 and $10 \times 10^{14} \text{ cm}^{-2}$. For the sample irradiated with 15 MeV electrons, TSC measurements were performed before and after isochronal annealing for 30 min at temperatures $T_{ann} = 80 - 280^\circ\text{C}$, in 20°C steps. At the other energies, data were only taken before and after

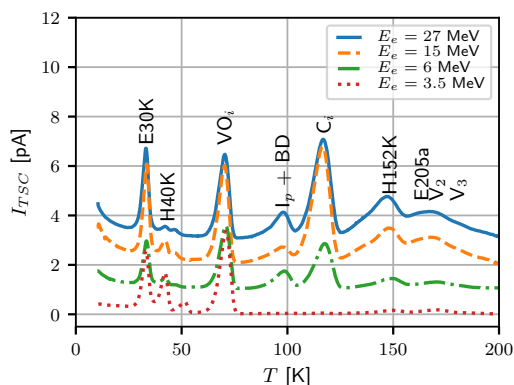


Figure 1: TSC spectra, $I_{TSC}(T)$, normalized to an electron fluence of $\Phi = 10^{14} \text{ cm}^{-2}$, after irradiation by electrons with different energies and annealing for 30 min at 80°C , measured at a heating rate of 0.183 K/s. The pad diodes were fabricated using standard float-zone silicon. For the trap filling forward-current injection has been applied at $T_0 = 10 \text{ K}$, so that both electron (E) and hole (H) traps contribute to $I_{TSC}(T)$. For clarity, the individual curves are shifted vertically by 1 pA. For the identification and labeling of the individual defects we refer to [2] and references therein. The dark current, which starts to dominate above 200 K, is subtracted.

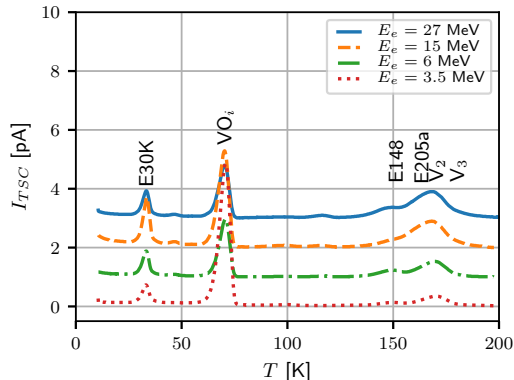


Figure 2: TSC spectra, $I_{TSC}(T)$, obtained after trap filling with light injection (with $\lambda = 520$ nm) through the 3.25 mm^2 window of the p^+ contact at $T_0 = 10$ K, for the same irradiation conditions and samples as the data shown in figure 1. As a result of the trap filling by light injection, only electron traps contribute to the TSC current. For clarity, the individual curves are shifted vertically by 1 pA.

annealing of 30 min at $T_{ann} = 80^\circ\text{C}$. For the TSC measurements the bias was applied to the back n^+ contact, and both p^+ contact and guard ring were at ground potential.

Figure 1 shows typical TSC spectra of pad diodes irradiated by electrons of different energies after 30 min annealing at 80°C . Trap filling has been applied at $T_0 = 10$ K with a forward-current of approximately 1 mA, so that both electron- and hole-traps are filled and contribute to the TSC spectra. The heating rate was $\beta = 0.183$ K/s. For more details we refer to [2, 5, 6]. In the following we will limit the discussion to the point defect VO_i (vacancy-oxygen interstitial) at 70 K and to the states in the 120 – 200 K region, which are known to be cluster defects and have a significant impact on the sensor performance [7].

For the TSC measurements analysed in this paper, the diodes were cooled to $T_0 = 10$ K at 200 V reverse bias to assure empty traps. At the temperature T_0 the traps were filled with electrons by injecting light of 520 nm through the 3.25 mm^2 window of the p^+ contact, and the current, I_{TSC} , released by the traps was recorded as a function of T for a constant heating rate $\beta = 0.183$ K/s. As a result of the light injection, only electron traps are filled and only the charges released from electron traps contribute to I_{TSC} (see figure 2).

3. Analysis Method

According to SRH statistics [8, 9] the temperature dependence of the TSC current, $I_{TSC}(T)$, from acceptor states at an energy E_a from the conduction band, which are filled with electrons at the temperature T_0 to the concentration N_t , is given by:

$$I_{TSC}(T) = \frac{A \cdot d \cdot q_0}{2} \cdot e(T) \cdot f_t(T) \cdot N_t, \quad (1)$$

$$e(T) = \sigma \cdot v_{th}(T) \cdot N_C(T) \cdot \exp\left(-\frac{E_a}{k_B T}\right), \quad (2)$$

$$f_t(T) = \exp\left(-\frac{1}{\beta} \int_{T_0}^T e(T') dT'\right), \quad (3)$$

with the elementary charge q_0 , the diode volume where the traps have been filled $A \cdot d$, the emission rate $e(T)$, the ratio of filled states at the temperature T relative to T_0 , $f_t(T)$, the thermal velocity of electrons $v_{th}(T)$, the electron capture cross-section σ , and the density of states at the conduction band $N_C(T)$. For these quantities the default values of Synopsys TCAD [10], in particular the

relation $v_{th}(T) = \sqrt{8 \cdot k_B T / (\pi \cdot m_{th}(300 \text{ K}))}$ of [11], are used. The effective thermal electron mass $m_{th}(300 \text{ K}) = 0.278 \cdot m_e$, with the Boltzmann constant k_B and the free electron mass m_e .

For point defects a constant value for E_a is expected. As proposed in [12], cluster defects can be characterized by an occupation-dependent value of $E_a(f_t)$. For the dependence $E_a(f_t)$, i. e. the change of the ionisation energy with the fraction f_t of defects filled in a cluster, a linear dependence is assumed:

$$E_a(f_t) = E_0 - \Delta E_a \cdot f_t. \quad (4)$$

The schematic drawing of figure 3 shows the potential energies of electrons in a cluster of 15 equally spaced electron traps on a straight line. The full dots correspond to $f_t = 1$, when all 15 traps are filled with electrons. The empty circles is the situation $f_t \rightarrow 0$, when only a single trap is filled and the energy is equal to the energy of the single isolated trap. The ionisation energy $E_a = E_0 - \Delta E_a$ is minimal for $f_t = 1$, and reaches its maximum $E_a = E_0$, the value for point defects, for $f_t \rightarrow 0$.

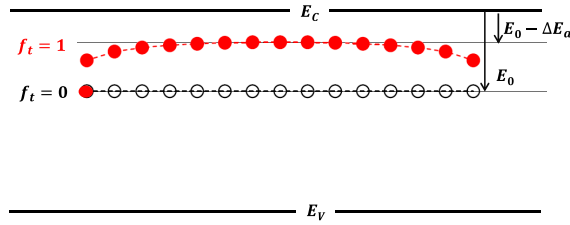


Figure 3: Schematic presentation of the potential energy of the electrons in a cluster consisting of 15 point defects equally spaced on a straight line. E_V denotes the edge of the valence band and E_C of the conduction band. The filled dots show the ionisation energies for the individual defects, when all traps are filled. The electron occupying the central defect has the lowest ionisation energy, $E_0 - \Delta E_a$. It will discharge first, when the sample is heated in the TSC measurement. The open circles correspond to the ionisation energy when only one state is filled with an electron. Its value is E_0 , the ionisation energy of the point defects, which build the cluster.

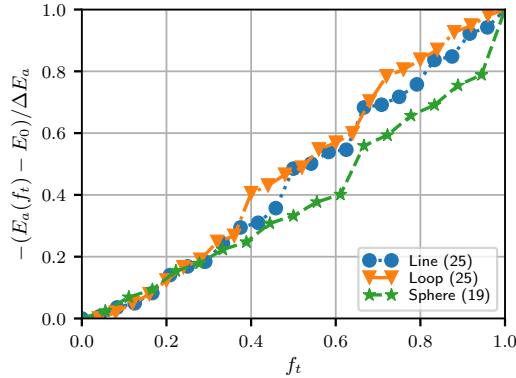


Figure 4: Simulated dependence of $E_a(f_t)$ for different cluster topologies. Line (25): 25 equally spaced point charges on a line, Loop (25): 25 equally spaced point charges on a circle, and Sphere (19): 19 point charges in a sphere on an equally spaced 3D-grid.

Figure 4 shows the results of simple, electrostatic simulations of the dependence of $E_a(f_t)$. For *Line* (25) the cluster is assumed to be a straight line of 25 equally spaced point defects, fixed in space. The energy difference between the conduction band and a single point defect is E_0 . In the initial state, $f_t = 1$, each point defect is occupied by an electron and negatively charged. The point defect with the highest (negative) potential energy, $-\Delta E_a$, and thus the lowest E_a value, $E_a = E_0 - \Delta E_a$, is discharged first, when the temperature is raised in the TSC measurement. Next, the point defect with the lowest E_a value for the new charge configuration is found and discharged.

This chain is continued, until all defects are discharged. The cluster *Loop* (25) consists of 25 equally spaced point defects on a circle, and *Sphere* (19) of 19 point defects in a sphere on a 3-D Cartesian grid. Figure 4 shows that to a good approximation for all three topologies, $E_a(f_t)$ is linear in f_t . Loop clusters are discussed in [12], which actually triggered our studies.

The data analysis consists in subtracting from the measured TSC current the dark current, obtained from the TSC measurement without trap filling. Then χ^2 -fits of eq. 1 for different T intervals are performed. For the errors 1% times the measured currents have been assumed, which takes into account the uncertainty of the current measurement as well as the accuracy of the temperature regulation of the TSC setup. The free parameters of the model are N_t , E_0 , ΔE_a and σ for each defect, where N_t is the density of point defects per volume, which are filled in the experiment at T_0 , i.e. the product of cluster density times the number of filled point defects in a cluster.

4. Results

4.1. The VO_i defect

As a first step, the vacancy-oxygen (VO_i) defect located at approximately $T = 70$ K is investigated. The VO_i is known to be a point defect. According to reference [13] it is an electron trap with an energy $E_0 = 176$ meV from the conduction band and an electron capture cross-section $\sigma = 79 \times 10^{-16}$ cm $^{-2}$. The values in reference [14] are $E_0 = 169$ meV and $\sigma = (100 \pm 10) \times 10^{-16}$ cm $^{-2}$. In figure 5 the TSC data after electron irradiation with $E_e = 27$ MeV to the fluence $\Phi = 4.3 \times 10^{14}$ cm $^{-2}$ and 30 min annealing at 80°C are shown as dots. The fit results are shown as a solid line, and the parameters are given in table 1. For the assumed 1% uncertainty for the I_{TSC} measurement, a $\chi^2 = 25$ for $NDF = 47$ degrees of freedom is found. We note that the differences *fit - measured* are dominated by the systematics of the temperature regulation and not by the statistical fluctuations of the current measurement. The values $E_0 = 166.1 \pm 0.7$ meV and $\sigma = (20 \pm 2) \times 10^{-16}$ cm $^{-2}$ (statistical errors only) differ significantly from the values given in [13]. If $E_0 = 176$ meV is assumed, the χ^2 increases to 61 and $\sigma = 80 \times 10^{-16}$ cm 2 is obtained. However, the value of $\Delta E_a = 0.88 \pm 0.03$ meV is incompatible with zero, the value expected for a point defect. For the remaining curves of figure 5 the value $E_0 = 166.1$ meV is assumed and ΔE_a is fixed to the values given in the insert. Values significantly larger than zero are incompatible with the data. We conclude that ΔE_a values, which differ significantly from zero are excluded.

The data after irradiation by electrons with energies E_e between 3.5 and 15 MeV and after 30 min annealing at 80°C, have also been analysed. In all cases, ΔE_a values close to zero and

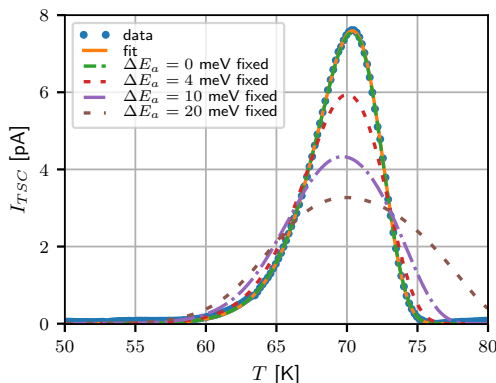


Figure 5: The measured TSC current after light injection at $T_0 = 10$ K (dots) for the point-like vacancy-oxygen defect (VO_i) after electron irradiation with $E_e = 27$ MeV to the fluence $\Phi = 4.3 \times 10^{14}$ cm $^{-2}$. For the fit (solid line) in the range $T = 64.5$ K to 74.0 K, the activation energy E_0 , N_t , σ , and ΔE_a are free parameters. The values $E_0 = 166.1$ meV and $\Delta E_a = -0.1$ meV are found. For the other fits E_0 is set to 166.1 meV, ΔE_a to the values given in the insert, and N_t and σ are free parameters.

E_0 [meV]	ΔE_a [meV]	$N_t/10^{12}$ [cm $^{-3}$]	$\sigma/10^{-16}$ [cm 2]	χ^2/NDF
166.1 ± 0.7	-0.1 ± 0.1	3.44 ± 0.01	19.7 ± 2.2	25/47
176	0.88 ± 0.03	3.43 ± 0.01	80.0 ± 0.2	61/48

Table 1: Results of the fits to I_{TSC} in the temperature range 64.5 to 74.0 K for the diode irradiated to the fluence of $\Phi = 4.3 \times 10^{14}$ cm $^{-2}$ by electrons with $E_e = 27$ MeV. The first row gives the results for the fit with E_0 left free, and the second line the fit with E_0 constrained to the value from reference [13].

consistent values for E_0 and σ are obtained. This confirms that VO_i is a point defect, and validates the analysis method for an isolated point defect.

4.2. Cluster defects

Next, the region $T = 120 - 200$ K is investigated, where overlapping defect clusters are located, which are responsible for part of the generation current, charge trapping and changes in the effective space-charge density [3]. The TSC spectra for the irradiations at the different E_e values after 30 min annealing at 80°C are shown in fig. 6.

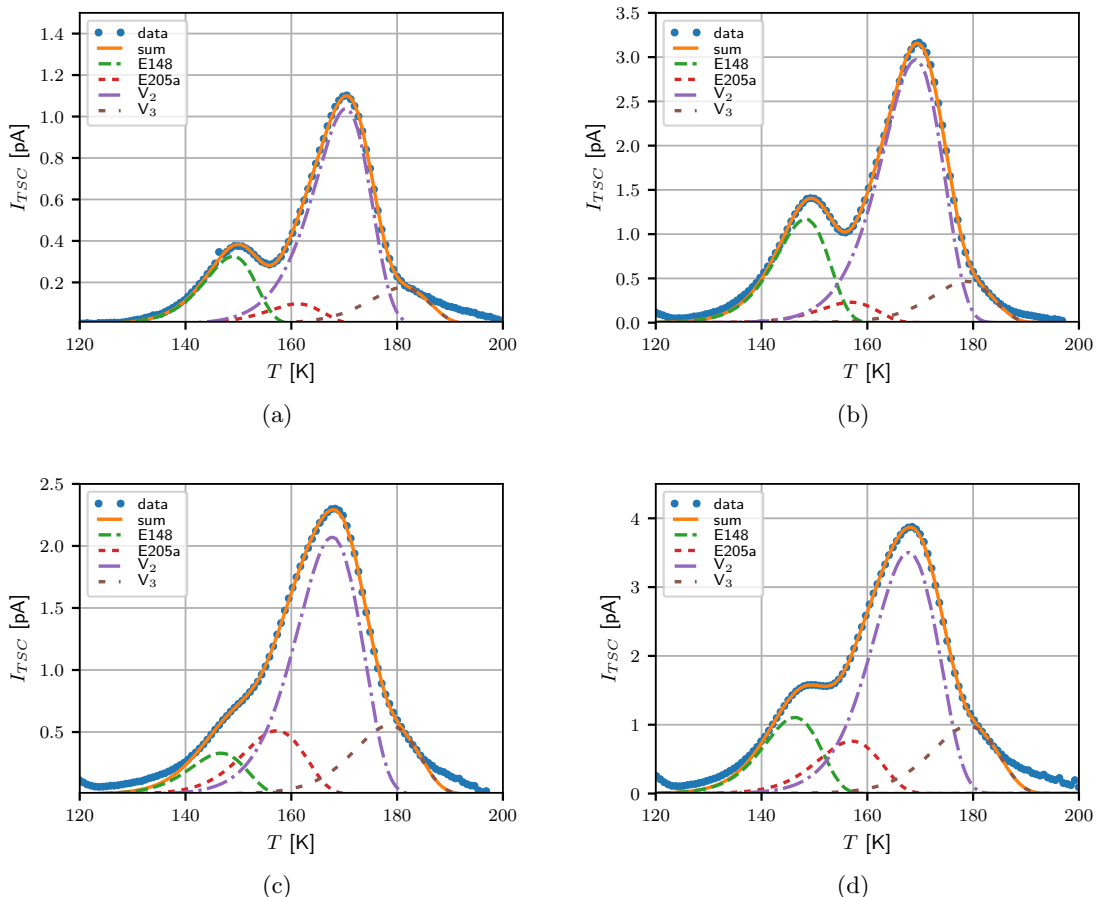


Figure 6: TSC spectra after 30 min annealing at 80°C with the fits described in the text for the temperature interval $T = 144.1 - 184.6$ K and irradiations with electrons of energies (a) 3.5 MeV, (b) 6 MeV, (c) 15 MeV, and (d) 27 MeV.

To describe the data, four defects have been assumed: the di-vacancy V_2 , the tri-vacancy V_3 and two additional defects, E148 and E205a. The values of E_0 from the literature are given in

Defect	E_0 [meV]	Ref.	ΔE_a [meV]	$N_t/10^{12}$ [cm $^{-3}$]	$\sigma/10^{-16}$ [cm 2]
E148	359	[5, 15]	4.3	0.33	4.6
E205a	393	[5, 13]	7.6	0.56	6.1
V $_2$ (-/0)	424	[13]	7.6	2.44	7.0
V $_3$ (-/0)	456	[3, 13]	4.3	0.65	9.7

Table 2: Parameters for the four electron traps in the $T = 120 - 200$ K region: E_0 is the energy distance of the isolated point defects from the conduction band taken from the reference given in the third column. ΔE_a , N_t and σ are the cluster-related energy shifts, the density of traps filled at T_0 and the electron cross-sections obtained from the fit for $T = 144.1 - 184.6$ K of eq. 1 to the data for $E_e = 15$ MeV after 30 min annealing at 80°C . The statistical errors are about 0.1 meV for ΔE_a and at the few % level for N_t and σ . The systematic uncertainties, e. g. from the choice of the fit interval, are significantly larger.

table 2. Using eq. 1 the sums of the contributions of all four defects have been fitted to the I_{TSC} measurements. In the fit, the literature values for E_0 , a ΔE_a value common for the two defects E148 and V $_3$, and another ΔE_a value common for E205a and V $_2$, have been assumed. Other assumptions, e. g. a common ΔE_a value for all 4 states, gave qualitatively similar results. Without such constraints, which are only poorly motivated, the fits do not converge to stable results. Figure 6 compares the fit results to the data, and table 2 shows as an example the parameters derived for the $E_e = 15$ MeV data. The TSC spectra are well described by the fits. It has been verified that they cannot be described with acceptable trap parameters if $\Delta E_a = 0$ is assumed, and conclude that the model with an occupation-dependent ionisation energy provides a good description of the TSC spectra of the cluster defects.

In order to investigate the dependence of the cluster formation on the electron energy, E_e , figure 7 shows $\Delta E_a(E_e)$ for the V $_3$ /E148 and the V $_2$ /E205a clusters obtained from the fits described above. The ΔE_a values for $E_e = 3.5$ MeV are compatible with zero. For higher electron energies the ΔE_a values differ significantly from zero and the energy dependence is as expected for a threshold of cluster formation in the region $E_e = 3.5 - 6$ MeV.

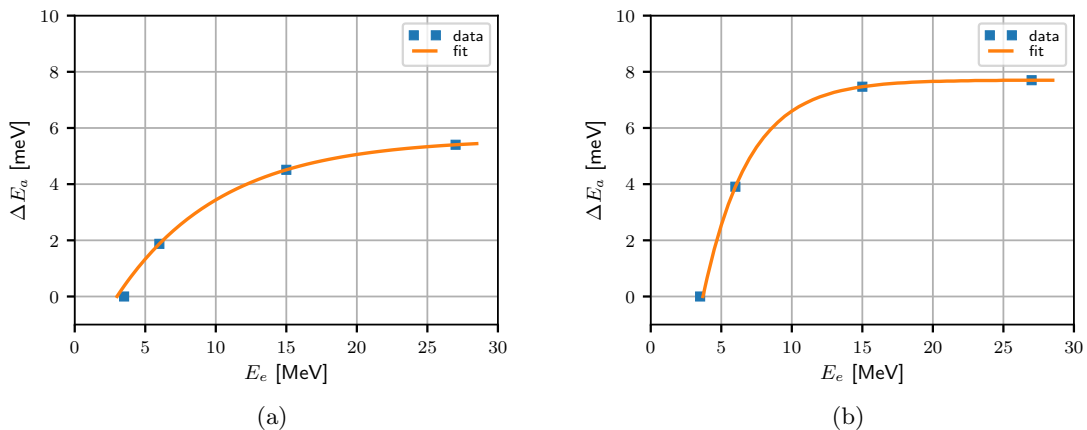


Figure 7: ΔE_a after 30 min annealing at 80°C as a function of electron energy, E_e , for (a) the E148/V $_3$ -, and (b) the E205a/V $_2$ -defect.

The phenomenological function with the free parameters B , γ_e and E_{th} ,

$$\Delta E_a(E_e) = B \cdot \left[1 - \exp\left(-\frac{E_e - E_{th}}{\gamma_e}\right) \right], \quad (5)$$

is fit to the $\Delta E_a(E_e)$ data. For the threshold values $E_{th}^{V_3/E148} = 3.0 \pm 0.5$ MeV and $E_{th}^{V_2/E205a} = 3.7 \pm 0.5$ MeV are obtained.

We note that for the models presented in section 3, a value of $\Delta E_a = 7.5$ meV corresponds to a spacing of about 100 nm of the point defects, which are filled at $T_0 = 10$ K in the clusters, to be compared to the silicon-lattice constant of 0.543 nm at 300 K. The values are compatible with simulations of electron-induced damage in silicon, which take into account the Mott cross-section, the vacancy and interstitial generation, as well as their diffusion and recombination [16].

4.3. Cluster annealing

In the following, the analysis of the data for the irradiation with $E_e = 15$ MeV for the conditions *as irradiated* and after isochronal annealing for $T_{ann} = 80 - 280^\circ\text{C}$ in 20°C steps and 30 min annealing time, is presented. The temperature history for *as irradiated* is only approximately known: After the 15 MeV irradiation at Dresden-Rossendorf the diode had been at room temperature for about eight hours during the transport to Hamburg, where it has been stored in the freezer at -25°C . In the following this condition is labeled $T_{ann} = 20^\circ\text{C}$. In figure 8 we show as examples the comparison of the fit results with the measurements for *as irradiated* and after the isochronal annealing steps of 80°C , 180°C and 280°C . For the fits the assumptions discussed in section 4.2 are made. For all T_{ann} values the data are well described by the model.

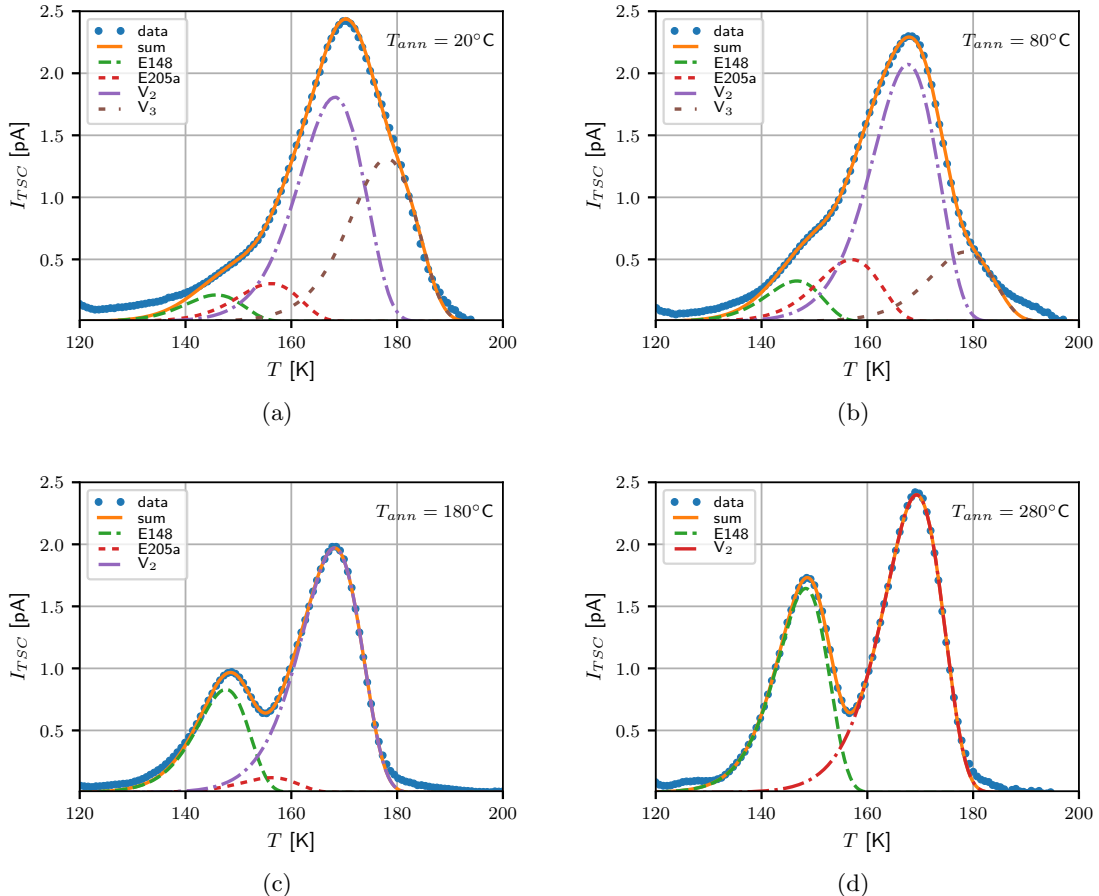


Figure 8: Measured TSC spectra, $I_{TSC}(T)$, and results of the fits assuming four defect clusters in the 120 – 200 K region for the diode irradiated by 15 MeV electrons to a fluence of $2.6 \cdot 10^{14} \text{ cm}^{-2}$ for (a) *as irradiated*, and after 30 min annealing at (b) 80°C , (c) 180°C , and (d) 280°C .

The results for N_t of the four defects, and the cross-sections for electrons, σ , as a function of T_{ann} are shown in figure 9. As discussed in section 3, N_t is not the density of filled clusters, but the product of the cluster density times the number of filled traps in the cluster. We observe

that with increasing annealing temperature N_t remains constant for V_2 , increases for E148, and vanishes for V_3 and for E205a. More details on the annealing behavior of V_3 and E205a can be found in [5]. As expected the electron cross-sections do not depend on T_{ann} .

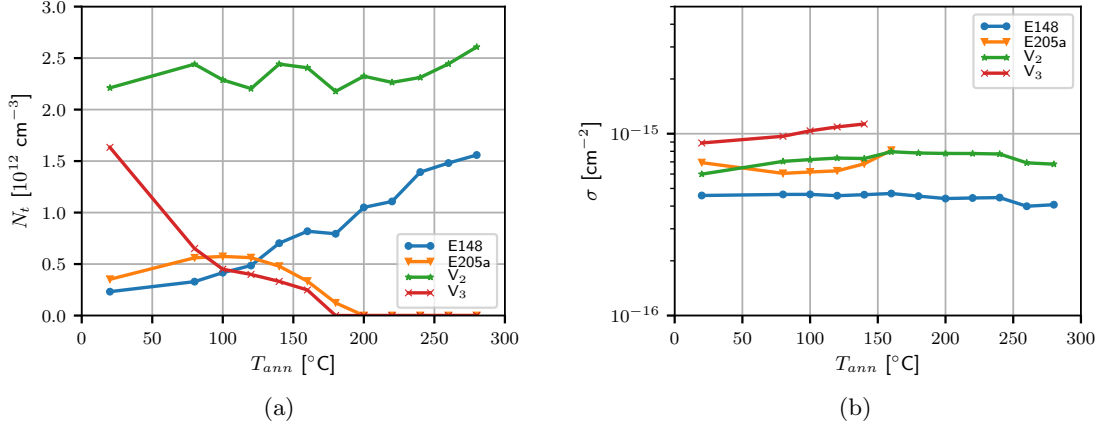


Figure 9: (a) Densities of traps filled at T_0 , N_t , and (b) electron cross-sections, σ , for the diodes irradiated by 15 MeV electrons to a fluence of $2.6 \times 10^{14} \text{ cm}^{-2}$ as a function of the annealing temperature, T_{ann} .

The results for ΔE_a as a function of T_{ann} for the traps $V_2/E205a$ and $V_3/E148$ are shown in figure 10. For $V_2/E205a$ the value of ΔE_a remains nearly constant ($\approx 7.5 \text{ meV}$) for the annealing at 80°C , then decreases to $\approx 2 \text{ meV}$ above 250°C .

For $V_3/E148$ the decrease of ΔE_a with T_{ann} is significantly faster, and a constant value of $\approx 1 \text{ meV}$ is reached at $T_{ann} = 140^\circ\text{C}$. For the description of $\Delta E_a(T_{ann})$ two models are introduced: a *first order decay model*, and a *diffusion model*.

The *first order decay model* uses the following formula for ΔE_a after the i -th annealing step

$$\Delta E_a(T_{ann}^{(i)}) = \Delta E_a(T_{ann}^{(i-1)}) \cdot e^{-k(T_{ann}^{(i)}) \cdot t_{ann}} \quad \text{with} \quad k(T_{ann}) = k_0 \cdot e^{-E_A/(k_B T_{ann})}, \quad (6)$$

with the annealing time $t_{ann} = 30 \text{ min}$. The first order process is described by the frequency factor k_0 and the activation energy E_A . For $\Delta E_a(T_{ann}^{(0)})$ the *as irradiated* data assigned to $T_{ann} = 20^\circ\text{C}$ are used. The results of the fits to the data are shown in figure 10 and in table 3. The model provides an acceptable description of the data.

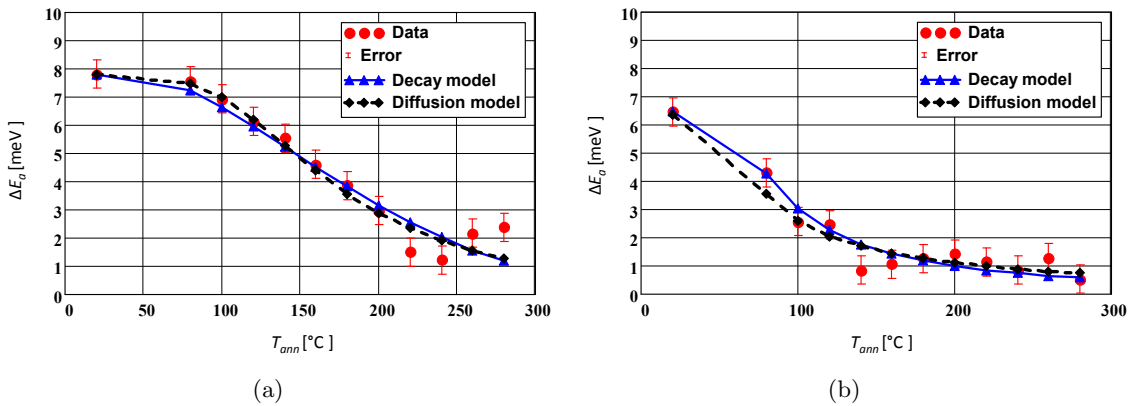


Figure 10: Dependence of $\Delta E_a(T_{ann})$ for the diode irradiated by 15 MeV electrons to a fluence of $2.6 \times 10^{14} \text{ cm}^{-2}$ for *as irradiated*, plotted at $T_{ann} = 20^\circ\text{C}$, and after isothermal annealing at the temperature T_{ann} for 30 min. The points with error bars are the data, the solid lines the fits by the *first order decay model*, and the dashed lines the fits by the *diffusion model* for (a) $V_2/E205a$ and (b) $V_3/E148$.

Defect	k_0 [1/s]	E_A [eV]	χ^2/NDF	Fit range [°C]
V ₂ /E205a	1.6×10^{-3}	0.113	15.6/10	20 – 280
V ₂ /E205a	42×10^{-3}	0.225	1.2/8	20 – 240
V ₃ /E148	7.2×10^{-6}	-0.105	7.9/10	20 – 280
V ₃ /E148	3.6×10^{-4}	0.014	2.3/3	20 – 140

Table 3: Parameters obtained for the fit of the *first order decay model*, equation 6, to the $\Delta E_a(T_{ann})$ results shown in figure 10. The last column gives the T_{ann} range of the fit

Defect	$D_{423.15K}$ [nm ² /s]	E_D [eV]	d_0 [nm]	σ_0 [nm]	χ^2/NDF	T_{ann} [°C]
V ₂ /E205a	6.3	0.423	27	159	6.4/8	20 – 280
V ₃ /E148	60	0.146	27	200	5.7/8	20 – 280

Table 4: Parameters obtained for the *diffusion model* described in the text, to the $\Delta E_a(T_{ann})$ results shown in figure 10.

The *diffusion model* follows a similar approach as the model discussed in section 3, which was used to derive the linear dependence of the ionisation energy on the fraction of occupied defects. Each cluster is assumed to consist of n_{clu} point defects, which diffuse during the annealing steps. For the temperature dependence of the diffusion constant the standard parametrisation

$$D(T) = D_0 \cdot e^{-E_D/(k_B T)} \quad (7)$$

is used. The activation energy for the diffusion of the point defects in the cluster is E_D , and D_0 a constant. For the fit n clusters with n_{clu} point defects each, are generated. The position of the j -th point defect in the k -th cluster after the $(i-1)$ -st annealing step is denoted by $\vec{x}_{j,k}^{(i-1)}$. The position after the i -th annealing step is $\vec{x}_{j,k}^{(i)} = \vec{x}_{j,k}^{(i-1)} + \delta\vec{x}$, where $\delta\vec{x}$ is a vector of three Gauss-distributed random numbers with width $\sigma_D(T_{ann}^{(i)}) = \sqrt{2 D(T_{ann}^{(i)}) \cdot t_{ann}}$. Assuming that all point defects are occupied by electrons, the individual potential energies $V_{j,k}^{(i)}$ are calculated. The biggest $|V_{j,k}^{(i)}|$ is assumed to be the ΔE_a value of the k -th cluster, and the average ΔE_a of the n clusters is fitted to the data. The initial positions of the point charges in the $\vec{x}_{j,k}^{(0)}$ are generated as n_{clu} points spaced by d_0 on a straight line each smeared with a vector of three Gauss-distributed random numbers with width σ_0 . For a given number of clusters, n , and cluster size, n_{clu} , the free parameters of the fit are σ_0 , d_0 , D_0 and E_D . For the fits to the data shown in figure 10, $n = 1000$ and $n_{clu} = 15$ are used. Fits have also been performed for other n_{clu} values. The χ^2 values obtained depend only weakly on n_{clu} and there is a shallow minimum around $n_{clu} = 15$. The parameters obtained from the fit are given in table 4, where the diffusion constants at 423.15 K, $D_{423.15K} = D_0 \cdot e^{-E_D/(k_B \cdot 423.15K)}$, instead of D_0 are shown. Using the value of D at the average annealing temperature 423.15 K has the advantage that $D_{423.15K}$ and E_D are essentially uncorrelated. In addition, it is more easily interpreted than D_0 , which corresponds to the value of D for $T_{ann} \rightarrow \infty$.

We note that, whereas the values of the parameters given in table 4 change significantly if the fit region is changed, the dependencies of $D(T_{ann})$ and $\sigma(T_{ann})$, shown in figure 11, are much less affected. The values of the diffusion activation energy $E_D \approx 0.42$ eV for V₂/E205a is similar to the value given in [17] for the vacancies V⁰ and V⁻¹, and $E_D \approx 0.15$ eV for V₃/E148 similar to the interstitial Si_i⁰.

As a pictorial presentation of the diffusion of the point defects in the clusters, figure 12 shows for the V₂/E205a cluster the $x-z$ distribution of the superposition of 20 cluster with 15 point defects each, using the parameters of table 4 for the conditions *as irradiated*, and after the annealing steps $T_{ann} = 80^\circ$, 180° and 280° C. The point defects of the initial cluster, which are separated by the distance d_0 , are generated along the z direction. As expected from figure 11b, hardly any diffusion is observed at $T_{ann} = 80^\circ$ C, the width increases by about a factor 3 at 180° C, and the clusters

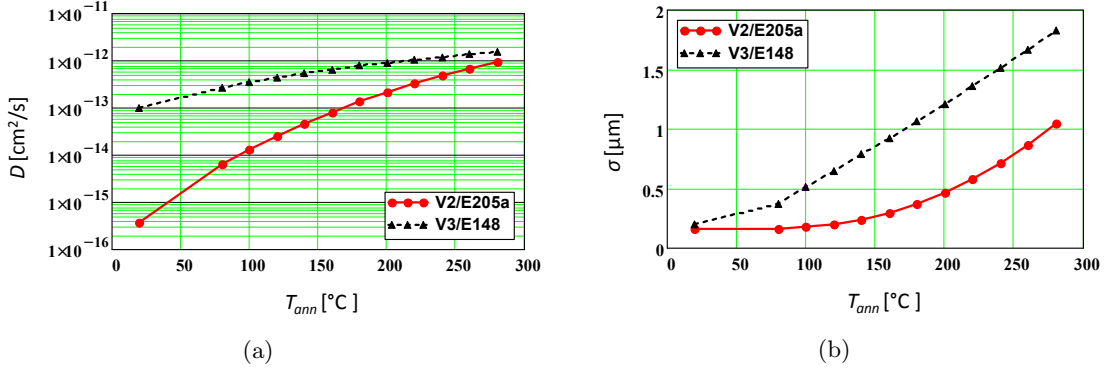


Figure 11: Results from the fits of the *diffusion model* for clusters containing $n_{clu} = 15$ point defects as a function of the temperature T_{ann} of 30 min isochronal annealing for the diode irradiated to a fluence of $2.6 \times 10^{14} \text{ cm}^{-2}$. (a) Diffusion constant, and (b) σ parameter of the Gaussian describing the diffusion of the point defects in the clusters.

are essentially dissociated at 280°C . We note that for $N_t = 2.5 \times 10^{12} \text{ cm}^{-3}$, shown in figure 9a, and 15 point defects in each cluster, the average distance between clusters is $\approx 2 \mu\text{m}$.

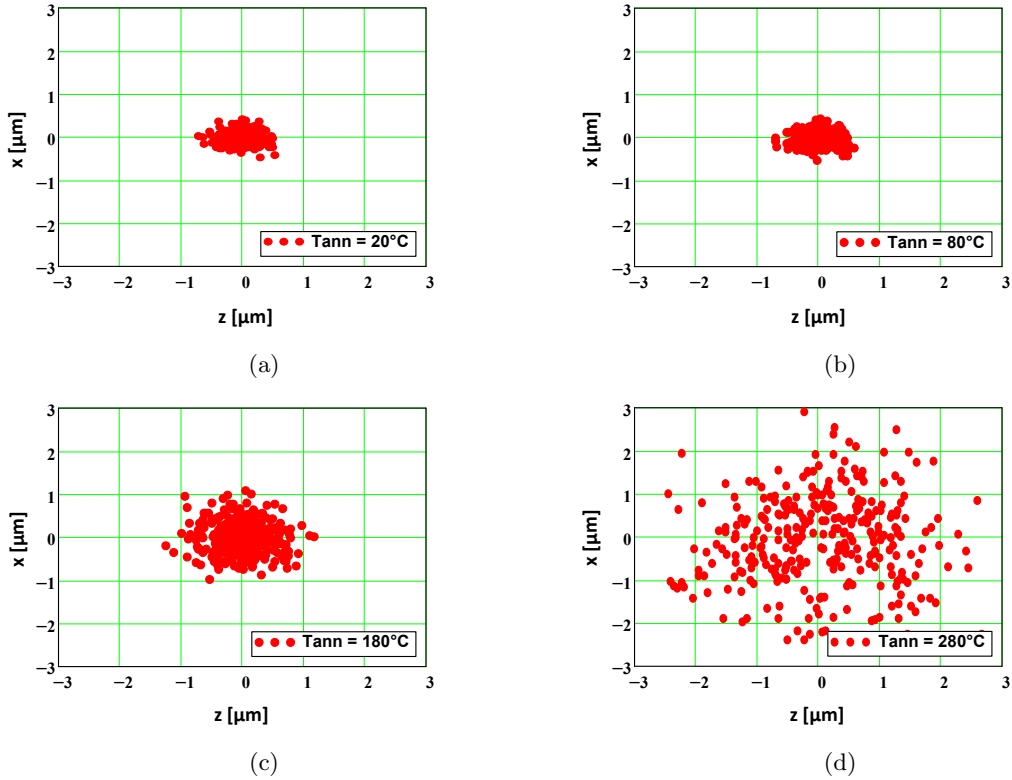


Figure 12: Diffusion of the point charges in the $V_2/E205a$ cluster simulated using the parameters of table 4 for (a) *as irradiated*, and after 30 min annealing at (b) 80°C , (c) 180°C , and (d) 280°C . To illustrate the diffusion, for the presentation 20 clusters of 15 point charges each are superposed.

We now summarise the results of the two models used to describe the annealing measurements: Both models provide a description of the dependence $\Delta E_a(T_{ann})$ for the $V_2/E205a$ and the $V_3/E148$ clusters. Whereas the *first order decay model* is a purely phenomenological parametrisation, the *diffusion model* is physics based and gives, within the assumptions made to determine the ΔE_a values and the limitation of this simple model, insight into the cluster annealing. The

diffusion-activation energy, E_D , is quite different for the two cluster defects: ≈ 0.4 eV for $V_2/E205a$ and ≈ 0.15 eV for $V_3/E148$. At an annealing temperature of 80°C the diffusion parameter, D , for $V_2/E205a$ is about a factor 50 smaller than for $V_3/E148$. However at 280°C , the highest annealing temperature investigated, they are quite similar. As a consequence, the diffusion of the point defects in the $V_3/E148$ cluster becomes significant only for temperatures above 150°C , whereas for the $V_2/E205a$ cluster it is already significant at room temperature. At the highest annealing temperatures the spread of the points in the cluster approaches the average distance between the clusters.

5. Conclusions

In this paper a new method of analyzing TSC (Thermally Stimulated Current) spectra of radiation-damaged silicon diodes is presented. It is based on the Shockley-Read-Hall statistics and can be used to describe both point and cluster defects. An ionisation energy, E_a , which depends on f_t , the fraction of filled point defects in the cluster, is introduced. Simple electrostatic model calculations show that a linear dependence $E_a(f_t) = E_0 - \Delta E_a \cdot f_t$ appears to be a reasonable approximation, where E_0 is the ionisation energy of the point defect which makes up the cluster, and ΔE_a the difference in ionisation energy between $f_t \rightarrow 0$ and $f_t = 1$. The method is applied to the analysis of TSC spectra from n-type silicon diodes irradiated by electrons in the energy range between 3.5 and 27 MeV. For the filling of the traps the p^+ implants of the diodes are exposed to green light, so that only acceptor traps contribute to the TSC current.

As a first step the VO_i defect (an electron trap with $E_0 \approx 0.17$ eV, which is known to be a point defect) is analysed for the diode irradiated by 27 MeV electrons to a fluence of $4.3 \times 10^{14} \text{ cm}^{-2}$. The value found for ΔE_a is compatible with zero. This confirms that VO_i is a point defect, and also demonstrates the validity of the method for point defects.

Next, the radiation-induced deep acceptor states with energies between 0.35 and 0.46 eV from the conduction band are investigated. They are responsible for part of the generation current, for charge trapping and for changes of the effective space-charge density with irradiation. In the analysis it is assumed that four defects, E148, E205a, V_2 , and V_3 contribute to the TSC current in this energy region. For the fits to the TSC spectra, the ionisation energies from the literature and common ΔE_a values for V_2 and E205a as well as for V_3 and E148 had to be assumed. Without these or similar not too well justified assumptions, the fits do not converge to stable values.

To study the dependence of the cluster formation on electron energy, the data for $E_e = 3.5, 6, 15,$ and 27 MeV after annealing for 30 min at 80°C are analysed. For the lowest electron energy $\Delta E_a = 0$, whereas for the higher electron energies positive ΔE_a values are found. After a rapid increase with electron energy, a tendency towards a saturation of ΔE_a is observed. This is taken as evidence for cluster formation above a threshold, which is somewhere between $E_e = 3.5 - 6$ MeV.

To study the annealing of the clusters, the data for the irradiation with 15 MeV electrons and the conditions *as irradiated* and after isochronal annealing for 30 min between $T_{ann} = 80 - 280^\circ\text{C}$ are analysed with the assumptions discussed above. For both $V_2/E205$ and $V_3/E148$, ΔE_a is found to decrease with T_{ann} , however the decrease for $V_3/E148$ is significantly faster than for $V_2/E205$. Two models, a *first order decay model* and a *diffusion model*, provide adequate descriptions of the data. Using the latter model the T_{ann} dependence of the diffusion parameters and of the spatial spread of the point defects in the cluster is estimated. It is found, that at $T_{ann} = 80^\circ\text{C}$ the diffusion constant for $V_2/E205a$ is about a factor 50 smaller than for $V_3/E148$, whereas at $T_{ann} = 280^\circ\text{C}$, they are quite similar. For the diffusion-activation energy, E_D , a value of 0.42 eV is determined for the $V_2/E205$ cluster, and 0.15 eV for the $V_3/E148$ cluster. For the highest T_{ann} values, the spread of the point defects in the clusters approaches the average distance between the clusters.

6. Acknowledgements

This work has been performed in the framework of the CERN-RD50 collaboration and PNII-ID-PCE-2011-3 Nr. 72/5.10.2011, and partially funded by CiS, the German BMBF and the Helmholtz

Alliance Physics at the Terascale. I. Pintilie and R. Radu gratefully acknowledge partial funding from the Romanian core program PN18-11 (funded by ANCSI). R. Radu was also partially supported by the Marie Curie Initial Training Network MC-PAD and the fellowship A127881 of the German Academic Exchange Service (DAAD). We also thank the teams at the irradiation facilities at the Belarusian State University at Minsk, the PTB at Braunschweig, and the ELBE accelerator at Dresden-Rossendorf, where the irradiations have been performed. We are grateful to P. Buhmann and M. Matyssek for maintaining the measurement infrastructure of the Hamburg Detector Laboratory, where the measurements were performed, in an excellent shape.

7. References

References

- [1] V. Eremin, E. Verbitskaya, Z. Li, The origin of double peak electric field distribution in heavily irradiated silicon detectors, *Nucl. Instr. & Meth. A* 476, 556 (2002).
- [2] R. Radu et al., Radiation damage in n-type silicon diodes after electron irradiation with energies between 1.5 MeV and 15 MeV, *Nucl. Instr. & Meth. in Phys. Res. A* 730, 84 (2013).
- [3] R. Radu et al., Investigation of point and extended defects in electron irradiated silicon: dependence on the particle energy, *J. Appl. Phys.* 117, 164503 (2015).
- [4] V. A. J. Lint, T. M. Flanagan, R. E. Leadon, J. A. Naber, and V. C. Rogers, *Mechanisms of Radiation Effects in Electronic Materials*, Vol. 1, John Wiley & Sons, Inc. (1980); p. 272 and p. 286.
- [5] A. Junkes, Influence of radiation induced defect clusters on silicon particle detectors, PhD Thesis, Hamburg University, DESY-THESIS-2011-031.
- [6] I. Pintilie et al., Stable radiation induced donor generation and its influence on the radiation tolerance of silicon diodes, *Nucl. Instr. & Meth. in Phys. Res. A* 556, 197 (2006).
- [7] I. Pintilie et al., Cluster related hole traps with enhanced-field-emission - the source for long term annealing in hadron irradiated Si diodes, *Appl. Phys. Lett.* 92, 024101 (2008).
- [8] W. Shockley and W. T. Read, Statistics of the recombinations of holes and electrons, *Phys. Rev.* 87, 835 (1952).
- [9] R. N. Hall, Electron-hole recombination in germanium, *Phys. Rev.* 87, 387 (1952).
- [10] Synopsys TCAD web-page, <http://www.synopsys.com>.
- [11] M. A. Green, Intrinsic concentration, effective densities of states, and effective mass in silicon, *J. Appl. Physics*, vol. 67-6, 2944–2954 (1990).
- [12] A. Scheinemann and A. Schenk, TCAD-based DLTS simulation for analysis of extended defects, *Phys. Stat. Sol. A* 2111, 136 (2014).
- [13] M. Moll, Radiation damage in silicon particle detectors, PhD Thesis, Hamburg University, DESY-THESIS-1999-040.
- [14] S.D. Brotherton and P. Bradley, Defect production and lifetime control in electron and γ -irradiated silicon, *J. Appl. Physics*, vol. 53-8, 5720 (1982).
- [15] I. Pintilie et al., Thermally stimulated current method applied to diodes with high concentration of deep trapping levels, *Applied Physics Letters*, vol. 78-4, 550 (2001).
- [16] G. Lindstroem and G. Kramberger, Electron Induced Damage in Silicon, presentation at the 24th RD50 Workshop, Bucharest 11–13 June 2014, unpublished.
- [17] S.M. Myers P.J. Cooper and W.R. Wampler, Model of defect reactions and the influence of clustering in pulse-neutron-irradiated Si, *J. Appl. Physics* 104, 044507 (2008).